

# Artificial Neural Network based prediction of Specific Fuel Consumption in various Compression Ratio CI Engine Fueled with Various Plastic Composition Pyrolysis oil and Diesel

<sup>[1]</sup>Maulik A. Modi, <sup>[2]</sup>Tushar M. Patel

<sup>[1]</sup>Research Scholar, Mechanical Engineering Department, KSV University, Gandhinagar, Gujarat, India

<sup>[2]</sup>Professor, Mechanical Engineering Department, LDRP-ITR, KSV University, Gandhinagar, Gujarat, India

\*Corresponding author: maulikmodi325@gmail.com

**Abstract:** This study looks at the usage of Artificial Neural Network Modeling for predicting Specific Fuel Consumption for compression ignition engines running on Diesel, Low-Density Polyethylene Pyrolysis Oil (LDPE PO), High-Density Polyethylene Pyrolysis Oil (HDPE PO), and Polypropylene Pyrolysis Oil (PP PO). Using preliminary practical findings, The Model of ANN was built to estimate SFC by adjusting the parameters of the engine. SFC is anticipated by adjusting the parameters and utilizing the orthogonal array. The experiment is then carried out using an orthogonal array. The outcomes of experimental work are used to create an ANN model. In the case of a non-linear mapping between input & output, the classic back-propagation method and a multi-layer perception network are utilized. The values of Mean Square Error (MSE), Root Mean Square Error (RMSE), and Regression Coefficient ( $R^2$ ) for LM10TP architecture are  $1.5143 \times 10^{-06}$ , 0.0012 & 1 in training & the validation values  $1.2185 \times 10^{-06}$ , 0.0011 and 0.9999 respectively. It was discovered that neural networks are useful tools for prediction since they performed well in specific fuel consumption prediction in both training and validation.

**Keywords:** high density polyethylene pyrolysis oil (hdpe po); low density polyethylene pyrolysis oil (ldpe po); polypropylene pyrolysis oil (pp po); artificial neural network; specific fuel consumption; compression ignition engine.

## 1. Introduction

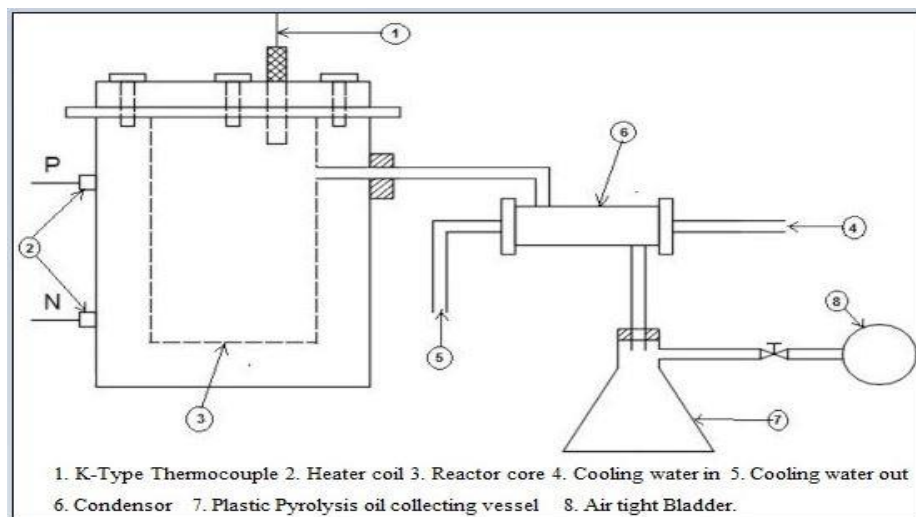
I have read hundreds of articles in newspapers about the major problem with plastic trash. In our society, it is common practice to toss away food in plastic bags, and animals searching for food get the food in plastic bags, and they consume food with plastic that is not digestible, and the storage of this plastic in their stomach leads to the development of cancer's cell in their bodies. The majority of plastic garbage ends up in landfills, where it forms a layer in the soil, due to the plastic layer preventing rainwater from reaching the required depth and crops from receiving sufficient nutrients from the soil. Storage of petroleum products is limited and as per the current usage; it will become empty in the nearest future, so required to find alternative options for petroleum products. The intermolecular structure of plastic material has a long chain of carbon and hydrogen and during the combustion of carbon can get energy. And in the current work with the help of the pyrolysis process fuel is generated from different types of waste plastic and used in Diesel engines and tested for emission and performance of the engine. In an engine using waste plastic fuel can reduce the waste plastic that goes into landfills, save the life of animals by awareness in society, and also satisfy the scarcity of petroleum products. For many decades, the diesel engine has dominated as a source of mechanical power, an engine useful in many fields such as industries, agriculture, and vehicles, among others. Because of the well-known fact that petroleum reservoirs are rapidly depleting, alternative fuel is the fastest-developing fuel replacement in the current environment (Cheikh et al. 2016). Because of human health hazards such as air pollution, acid rain, increased greenhouse gas emissions, and an unbalanced thermal balance of the planet caused by diesel

combustion, alternative fuels are a viable future energy source for businesses or transportation sectors. Given the aforementioned conflicts, it is critical to minimize emissions by limiting petroleum fuel usage. As a result, using environmentally acceptable, innocuous, ecological substitute fuels efficiently reduces the use of petroleum and emissions of greenhouse gas (Yinjie et al. 2018). Here a partial restoration of diesel with biodiesel in CI engines might result in a viable mix with attributes similar to base diesel (Dey, S., M. Deb, P. K. Das 2019). However, blending alcohol with diesel is usually a complex and difficult operation that needs a specialized solution. The fundamental disadvantage of such diesel-alcohol mixes is their instability (Shahir et al. 2014). Extensive and time-consuming testing is needed to evaluate the emission and performance characteristics of a CI engine. To address this, researchers used the properly trained with appropriate data, an ANN prophesy tool may forecast the true value with astonishing precision. As a result, little experimentation is necessary for an efficient and successful ANN model, and the produced data will be used to train the network. The ability of ANN to learn, represent non-linear processes, and adapt to changes in real time distinguishes it from other prediction technologies. The predictive power of ANNs for diesel engine performance metrics was explored (Parlak et al. 2006). ANN was used to forecast the emission and performance characteristics of hybrid fuels. They created a replica for training and assessing experimental data using a typical back propagation approach. They used the constructed network to predict engine characteristics with a little root mean square error (RMSE) and a correlation coefficient (R) of 0.975-0.999 (Wang et al. 2017). Created an ANN model to estimate NO<sub>x</sub>, torque and CO emissions from a CI engine running on peanut biodiesel, diesel and peanut biodiesel alcohol blend. The back propagation method has more accurate outcomes than standard regression modeling (Tosun et al. 2016). Injection time, compression ratio, blend percentage, and % load were used as input factors to estimate exhaust gas temperature (EGT), smoke, UHC emissions, brake thermal efficiency (BTE), brake specific energy consumption (BSEC), NO<sub>x</sub>. They discovered a significant connection between experimental and ANN-predicted values with 8% mean relative error (MRE) (Pai, P. Srinivasa, and BR Shrinivasa Rao 2011). For engine performance, specific fuel consumption (SFC), and exhaust emissions (CO and HC), Waste-cooking biodiesel with replica of ANN was also explored. Using MLP network, they obtained good correlation coefficients (R) of 0.999, 0.999, 0.9487, 0.929, and for HC emissions, SFC, engine torque, CO respectively (Oguz, Hidayet, Ismail Saritas, and Hakan Emre Baydan, 2010). An ANN prophecy art was also created for predicting various performance parameters of diesel biodiesel-bioethanol blends, and it was revealed that ANN is acceptable for predicting various performance parameters with a 99.94% dependability value (Ghobadian et al. 2009). Based on the lowest MSE value of 0.0001086 at 18 hidden neurons, the ANN technique is utilized to estimate exhaust pollutants such as soot, NO<sub>x</sub>, and CO<sub>2</sub> (Javed et al. 2015). A solid model for predicting various engine operating characteristics. They found an accurate match between experimental and projected data using the ANFIS model, with high overall R (0.998875-0.999989) and 0.08-1.84% MAPE value (Roy et al. 2015). The statistical errors of ANN training on various network topologies were also investigated, and an optimal network design was for the prediction of output parameters within range. Using the developed model with 6 neurons in the hidden layer, they obtained MSE, MAPE and R values of 0.000225, 2.88%, 0.99893, and respectively. However, in the domain of diesel-biodiesel-ethanol blends for diesel engine applications (Bhowmik et al. 2017). Experiment findings reveal that increasing IOP causes increased HRR and decreased NO<sub>x</sub> levels. The average rise in BTHE was 4%, whereas NO<sub>x</sub> levels were lowered by 9%. UBHC and CO emissions were reduced by 33% and 10.5%, respectively (Srinidhi et al. 2022). The performance of the nano particles-induced NB25 mix is superior to EGR. BTE was raised by 17% using the nanoparticle approach. Even though the EGR approach efficiently lowers nitrogen oxide emissions, far larger quantities of unburned HC, CO, and CO<sub>2</sub> were found (Srinidhi et al. 2022). A CI Engine fed with NB25 and fuel additives were evaluated for performance and emissions. The findings show that when additives with NiO fuel were added to the NB25 mix, high NO<sub>x</sub> peaks with improved performance and lower CO and HC emissions were detected (Campili Srinidhi et al. 2021). The predicted and experimental responses of RSM predictors have a small error range of 0.7%-4.64% (Srinidhi et al. 2021). According to the results of the experiments, 75 ppm NiO in the NB25 blend lowers thermal NO<sub>x</sub> upto 6.2% when compared to the absence of nanoparticles, BTE improves by 2.9%, and BSFC decreases by 1.8%. The addition of 75 ppm NiO in NB25 resulted in not only the greatest performance but also the lowest hazardous emission (Campili et al. 2021). A feed-forward multi-layer is utilized in combination with Trainlm, a Levenberg-Marquardt backpropagation training technique. The best static injection

time, fuel injection pressure, and HnOME mix parameters were found to be 18, 22° bTDC, 227 bar, and B60 (Channapattana et al. 2017). At 240 bar IP, Honne biodiesel's BSFC is 0.042 Kg/kWhr greater than that of Diesel oil. As the IP and blend amounts grow, so do NOX emissions. The B20 blend outperforms other Honne biodiesel blends in terms of thermal performance, but it creates greater amounts of exhaust emissions (Channapattana et al. 2015). An experiment study of performance metrics (BP, BSFC, BTE, and EGT) and emission characteristics (NO<sub>x</sub>, HC, CO., etc.) on a modified variable compression ratio CI engine is obtained and compared with conventional diesel at various loads (Channapattana et al. 2015). An application of ANN modeling to forecast the SFC of a 4-Stroke single-cylinder diesel engine powered by Diesel. LDPE PO (Low-Density Polyethylene Pyrolysis Oil), HDPE PO (High-Density Polyethylene Pyrolysis Oil), and PP PO (Polypropylene Pyrolysis Oil). Based on preliminary experimental results, an ANN model was built to forecast SFC by altering the percentage of load, injection pressure, and compression ratio. In the current experimental work, four types of fuel are taken for testing purposes. 64 sets of experiments for each fuel required using an orthogonal array 16 sets of experiments of each fuel were chosen and performed experimental work, Using ANN method calculate the engine performance parameter for remaining and already chosen sets of an experiment. Also, compare experimental results with ANN predicted result for minimum mean square error. The current study intended to create an Experimental-ANN hybrid model for the particular fuel consumption of a Diesel Engine. The ANN model is constructed utilizing experimental data from specific fuel consumption models based on the L64 orthogonal array. Using a neural network model saves time and effort. The value of MSE and R<sup>2</sup> result in the training and validation model will require the nearest value of zero and one respectively. ANN finds the best prediction tool for optimization. Uncertainties in the experiment's numerous equipment and parameters taken as per literature survey (Channapattana et al. 2017).

## 2. Material And Methods




To generate waste plastic pyrolysis oil, many forms of plastic waste are utilized as raw materials in the pyrolysis process. Pyrolysis is the thermal breakdown of organic matter in the absence of oxygen. A closed container was selected inside the waste plastic filled then the heat was given from the bottom of the container, vapor of plastic waste cooled inside the condenser at the bottom of the condenser plastic pyrolysis oil was collected in a bottle of.





**Fig 1:** Pyrolysis oil production Experimental view

Figure 1 shows Pyrolysis oil production Experimental view in the experimental setup contains a pyrolysis chamber with a heat source and condenser. Different types of waste plastic feed into the combustion chamber to produce pyrolysis oil. Waste materials of Low-density polyethylene, High-Density polyethylene, and polypropylene are used to produce pyrolysis oil and tested with diesel fuel in engines. The parameters of diesel fuel and plastic pyrolysis fuel are listed in Table 1. The Taguchi method is a collection of mathematical and statistical techniques useful for the parametric optimization. ANN is used to study the connection between a response and a set of quantitative experimental variables or factors.

LDPE PYROLYSIS OIL Density = 765 kg/m <sup>3</sup> , LCV = 10530 Calorie/ (gm- <sup>0</sup> c)	HDPE PYROLYSIS OIL Density = 790 kg/m <sup>3</sup> , LCV = 9714 Calorie/ (gm- <sup>0</sup> c)	PP PYROLYSIS OIL Density = 736 kg/m <sup>3</sup> , LCV = 9901 Calorie/ (gm- <sup>0</sup> c)
		

**Fig 2:** Pyrolysis oil used in experiment

### 3. Experimental Methodology

**Table 1:** Fuel Properties Table

Sample/ Properti es	Acid Value	Specifi c Gravit y	Densit y	LCV	HCV	Flash Point	Fire Point	Viscosity@40 °C	Dynamic Viscosity@40 °C
Unit	(mg of KOH )/ gm of oil	-	kg/m <sup>3</sup>	Calori e/ (gm- °c)	Calori e/ (gm- °c)	°C	°C	cSt	Cp
ASTM Standard	D675 1	D287	D287	D4800 9	D4809	D9358 T	D9358 T	D445	D445
Diesel	0.6	0.83	830	10034	10619	53	56	2.09	1.73
LDPE PO	-	0.765	765	10530	11116	35	41	2.22	1.69
HDPE PO	-	0.79	790	9714	10300	31	37	1.86	1.47
PP PO	-	0.736	736	9901	10487	24	31	1.64	1.21

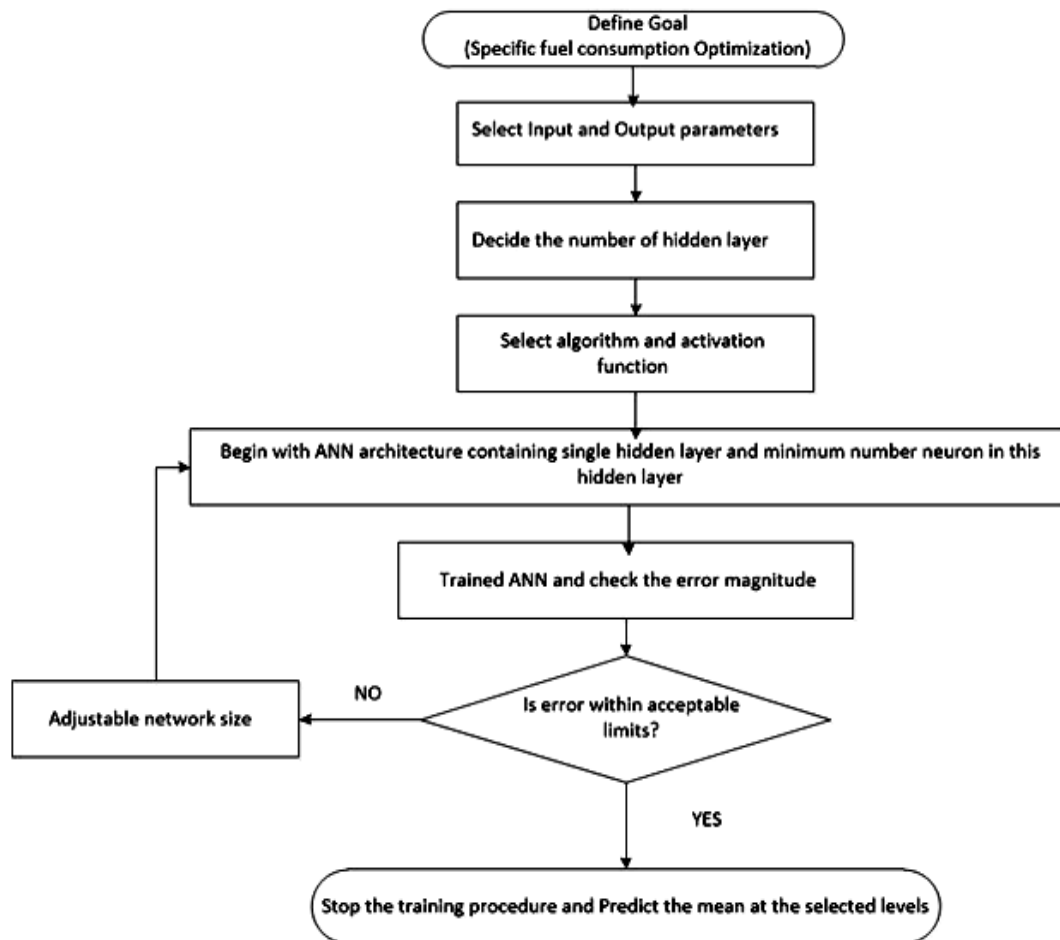


**Fig 3:** Flow chart of experiment (Patel & Bhatt, 2016)



Figure 3 depicts an experiment flow chart. Experiments for diesel, plastic pyrolysis fuel, injection pressure, and compression ratio are planned using Taguchi's L64 orthogonal array. Experimental work was performed with diesel and different types of plastic pyrolysis oil. Test engine specification taken as per literature review paper (Dey, S., M. Deb, P. K. Das 2019). Various injection pressure and compression ratios are used in the experimental setting. The photographic view to modify the compression ratio and injection pressure is shown in Figure 4.



**Fig 4:** Changing in Compression Ratio and Injection Pressure

**Table 2:** Factors and their levels

Factor	Level			
	1	2	3	4
Type of Fuel	1 (DIESEL)	2 (LDPE PO)	3(HDPE PO)	4 (PP PO)
Compression Ratio	15	16	17	18
Injection Pressure (bar)	180	200	220	240
Load (Kg)	0	4	8	12

Table 2 represents the factors and their levels taken into the experimental setup. Types of fuel, compression ratio, Injection pressure and Load considered. Every factor having four levels considered in experimental setup.

**Table 3:** Experimental Results Table

Sr. No	Experimental Run	Factors				SFC (kg/kWh)
		Types of fuel	CR	IP	Load	
Training Data Sets						
1	2	1	15	200	4.12	0.7631
2	3	1	15	220	8.13	0.4781
3	4	1	15	240	12.33	0.4092
4	5	1	16	180	3.88	0.7637
5	7	1	16	220	12.22	0.4414
6	8	1	16	240	0.13	15.9842
7	9	1	17	180	8.1	0.4814

8	11	1	17	220	0.23	8.2872
9	12	1	17	240	4.22	0.7088
10	13	1	18	180	12.25	0.4389
11	14	1	18	200	0.23	8.9635
12	16	1	18	240	8.22	0.4744
13	17	2	15	180	0.23	8.5068
14	18	2	15	200	4.25	0.6188
15	19	2	15	220	8.28	0.4642
16	21	2	16	180	4.22	0.5427
17	23	2	16	220	12.32	0.3997
18	24	2	16	240	0.17	11.7309
19	25	2	17	180	8.23	0.4458
20	26	2	17	200	12.42	0.3926
21	28	2	17	240	4.13	0.6368
22	29	2	18	180	12.33	0.3215
23	30	2	18	200	0.13	13.6036
24	32	2	18	240	8.21	0.4026
25	33	3	15	180	0.12	18.0943
26	35	3	15	220	8.13	0.4409
27	36	3	15	240	12.21	0.3952
28	37	3	16	180	4.23	0.7079
29	38	3	16	200	8.19	0.3935
30	40	3	16	240	0.23	9.3343
31	42	3	17	200	12.31	0.3746
32	43	3	17	220	0.14	14.2211
33	44	3	17	240	4.29	0.6267
34	45	3	18	180	11.73	0.4401
35	47	3	18	220	4.14	0.7291
36	48	3	18	240	8.22	0.4534
37	49	4	15	180	0.23	9.6329
38	50	4	15	200	4.13	0.6572
39	52	4	15	240	12.1	0.3296
40	54	4	16	200	8.12	0.3882
41	55	4	16	220	12.32	0.3167
42	56	4	16	240	0.26	8.5447
43	57	4	17	180	8.23	0.3843
44	59	4	17	220	0.24	8.3119
45	60	4	17	240	4.24	0.6332
46	61	4	18	180	12.11	0.3285
47	63	4	18	220	4.07	0.6896
48	64	4	18	240	8.31	0.3809
Validation Data Sets						
49	1	1	15	180	0.13	17.4198

50	6	1	16	200	8.23	0.4742
51	10	1	17	200	12.33	0.4206
52	15	1	18	220	4.22	0.7064
53	20	2	15	240	12.23	0.3440
54	22	2	16	200	8.11	0.4124
55	27	2	17	220	0.24	6.7708
56	31	2	18	220	4.33	0.5671
57	34	3	15	200	4.19	0.6044
58	39	3	16	220	12.35	0.3498
59	41	3	17	180	8.29	0.4878
60	46	3	18	200	0.15	14.3220
61	51	4	15	220	8.24	0.4005
62	53	4	16	180	4.23	0.6296
63	58	4	17	200	11.92	0.3070
64	62	4	18	200	0.2	9.9480

In Table 3 contained 64 experimental set up with specific fuel consumption performance parameter and in Table 4 shows the Experimental and BS-VI Emission range Comparison.

**Table 4:** Experimental and BS-VI Emission range Comparison

Emission Parameter	Fuel	Emission Range during Experiment	BS-VI Emission Range	Remarks
CO (%vol)	1 (DIESEL)	0.07-0.41	0.3	Only In overload out of Range
	2 (LDPE PO)	0.05-0.45		Only In overload out of Range
	3(HDPE PO)	0.09-0.33		Only In overload out of Range
	4 (PP PO)	0.07-0.26		Within Range
NO <sub>x</sub> (g/kWh)	1 (DIESEL)	0.239-4.493	88% Reduced compare with BS- IV 4.2	In overload out of Range
	2 (LDPE PO)	0.745-4.312		Only In overload out of Range
	3(HDPE PO)	0.205-4.167		Within Range
	4 (PP PO)	0.128-3.245		Within Range
HC (ppm)	1 (DIESEL)	15-52	200	Within Range
	2 (LDPE PO)	22-67		Within Range
	3(HDPE PO)	36-90		Within Range
	4 (PP PO)	31-260		Only In overload out of Range
Smoke (HSU)	1 (DIESEL)	1.8-24.5	26	Within Range
	2 (LDPE PO)	1.2-16.3		Within Range
	3(HDPE PO)	1.1-6.2		Within Range
	4 (PP PO)	0.8-26.5		Only In overload out of Range

#### 4. Effect Of Engine Parameter On Performance

The thermal efficiency and brake-specific fuel consumption rise as the compression ratio increases. Compression ratio increases result in greater in-cylinder pressure, quicker heat release, and shorter ignition delay. High-pressure fuel injection enhances fuel atomization, shortens the delay time, speeds up combustion,



and improves fuel/air mixing to promote full combustion, all of which increase fuel efficiency. With excessive injection pressure, the ignition delay time shortens, reducing the possibility of homogenous mixing and lowering combustion efficiency. Low injection pressure increases the diameter of fuel droplets, resulting in a longer ignition delay and inefficient combustion. The combustion parameters of an engine are affected by engine load. As engine load increases, engine speed lowers. When the load exceeds the rated load, the engine is overloaded. In an overload condition, the speed drops below the rated speed. Heavy loads have greater inertia and rolling resistance, both of which lead to higher fuel consumption. Overload puts a lot of strain on the system. The tyres might easily wear out and overheat. This results in costly tyre breakdowns and the risk of a disastrous blowout. Extra strain means the engine has to work harder to propel the car.

## 5. Effect Of Engine Parameter On Exhaust Emission

Lower exhaust gas temperatures were recorded at increased compression ratios. This is owing to improved heat-to-work conversion, which is caused by efficient combustion. The use of a lean mixture at part-load lowered exhaust gas temperature. Increasing the injection pressure resulted in quicker combustion, a considerable decrease in soot, especially at low engine speeds, but also a large increase in NO emissions, according to the data. The temperature of the exhaust gas rose with increasing engine load in all operating modes. This is related to higher fuel consumption, which causes an increase in total energy intake under high load. It was also determined that increasing the quantity of EGR. This orthogonal array was chosen because of its capacity to examine factor interactions. "Orthogonal arrays" (OA) are experimental designs that use specially created tables. The usage of these tables makes experiment design relatively simple and uniform. The value of specific fuel consumption is assessed to determine the appropriate injection pressure, compression ratio, and fuel. A series of experiments are carried out in order to determine the best injection pressure, compression ratio, and fuel. Because particular fuel consumption is deemed more relevant for study, an ANN model is developed to forecast specific fuel consumption using data from Table 4. Error Bars are a graphical addition that depicts the variability of data presented on a Cartesian graph. Error bars are used to illustrate estimated error or uncertainty in order to provide a broad idea of how exact a measurement is. In all the graphs of the current paper error bar is included.

## 6. ANN Model For Predicting Sfc Using Ann Approach

According to literature reviews, ANN models outperform regression models in terms of prediction capabilities. As a result, ANN models are constantly developed for predicting particular fuel usage. post-process model, Pre-processes, model simulation, training and design in the production of ANN prediction models are all covered in this part.

**Table 5:** Errors vs no. of neurons in hidden layer

No. of Neurons	MSE	R <sup>2</sup>
1	0.00173600	0.99733
2	0.00075035	0.99885
3	0.00032700	0.99950
4	0.00025842	0.99960
5	0.00015770	0.99988
6	0.00010799	0.99992
7	$5.0651 \times 10^{-06}$	0.99994
8	$8.545 \times 10^{-06}$	0.99995
9	$2.3233 \times 10^{-06}$	0.99999
10	$1.5143 \times 10^{-06}$	1
11	$4.1962 \times 10^{-06}$	1

12	$1.2958 \times 10^{-17}$	1
13	$2.1948 \times 10^{-16}$	1
14	$1.7804 \times 10^{-26}$	1
15	$4.0781 \times 10^{-24}$	1

Data must be translated into a range of -1 to 1 or 0 to 1 before being used for ANN training, i.e. normalised for ANN training. Range in [-1, 1], is used to determine data normalisation.

where:

$$x_n = 2 \times \left[ \frac{x - x_{\min}}{x_{\max} - x_{\min}} \right] - 1 \quad (1)$$

$x_n$  = Normalized Value of Variable  $x$ ;  $x$  = Value of Variable  $x$ ;  
 $x_{\min}$  = Min. Value of Variable  $x$ ;  $x_{\max}$  = Max. Value of Variable  $x$

Following normalisation, training target sets and input data are developed. Each input set, target data sets include normalised measured specific fuel consumption numbers. Study involves a function estimation or prediction problem where the eventual error reduction was to be as small as feasible. In the current experiment, each reading was obtained three times, and the average value of all three readings was used to calculate and construct graphs. During Experimental work, each minor precaution is taken to avoid a personal error. We have examined combustion charts for every experiment and the parameters responsible for the Acoustic signature and misfire are in a proper range. So, we did not experience any abnormal combustion during the experiment.

## 7. Neural Network Design

64 experimental data sets are separated into two categories: training and validation. MATLAB's Neural Network Toolbox is used to train and test multiple network configurations with varying numbers of hidden neurons. For training, 48 orthogonal array data employed & 16 data sets are chosen at random for validation. Training data reduce ANN learning processing time & boost model generalization. A maximum data used to train the models. Here, the Levenberg-Marquardt (LM) optimisation approach used to determine biases and weights. Training approach adjusts iteratively in order to remove errors between the objective & predicted output. The literature has shown that Levenberg-Marquardt can generate proper results quickly if the number of neurons in hidden layers is appropriately selected. Table 5 shows a performance analysis (MSE,  $R^2$ ) score that is equal to the no. of neurons in the hidden layer. With data Augmentation, Regularisation, Dropouts, Increasing the size of the training dataset, and Cross-validation, all mentioned ways to overcome overfitting, increasing the size of the training dataset was taken in the current work, for Training dataset 48 experiments, and Validation dataset 16 experiments.

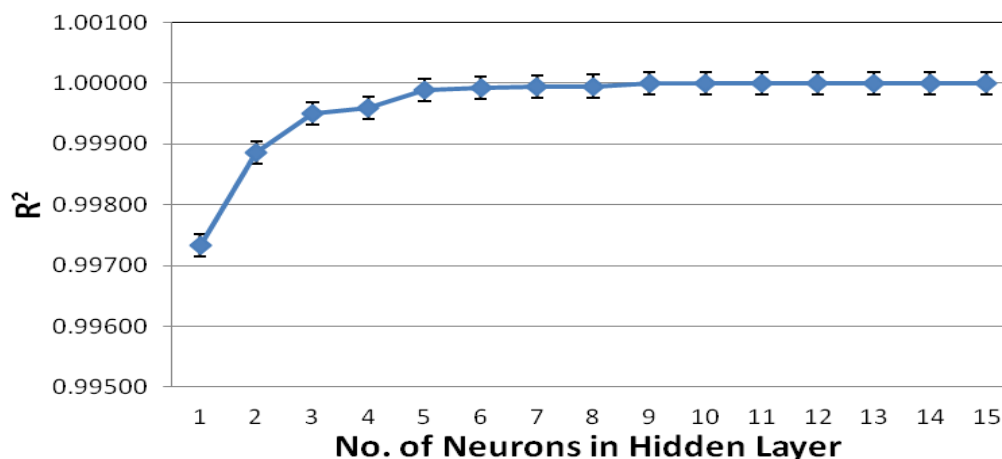
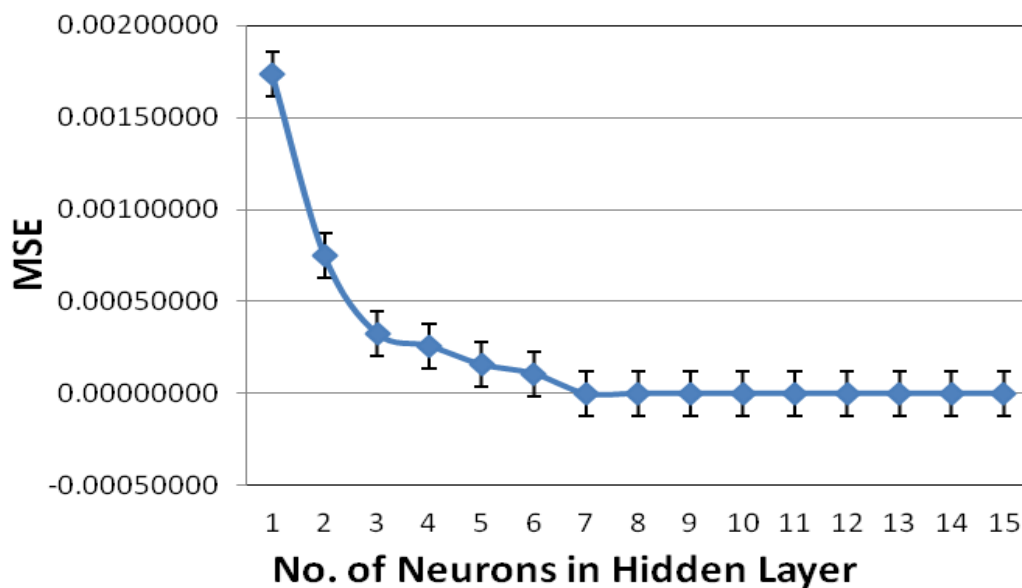
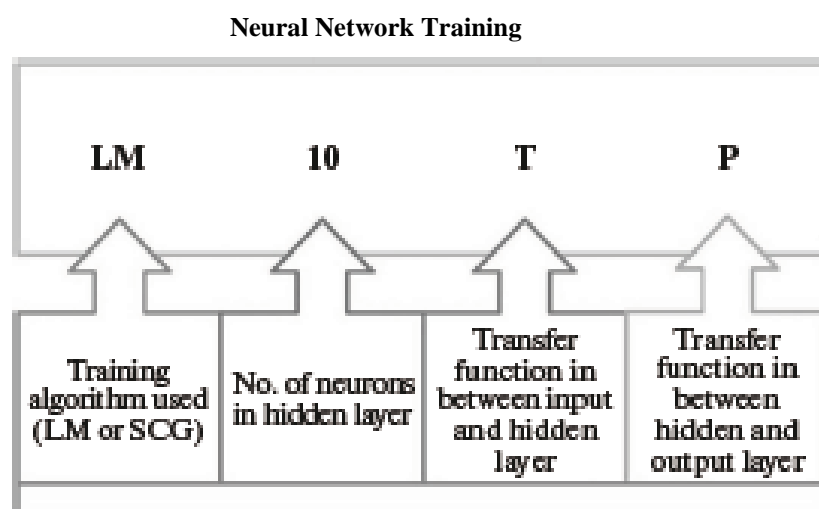


Fig 5:  $R^2$  vs. no. of neurons in hidden layer



**Fig 6:** No. of neurons vs MSE in hidden layer.

Figures 5 and 6 demonstrate how the number of neurons in the hidden layer affects  $R^2$  and MSE. When the number of neurons in the hidden layer reaches 10, the LM technique leads  $R^2$  to converge towards 1 and MSE to converge towards 0. However, in training, this algorithm overfits predicted data, preventing it from appropriately generalising. the network memorises training data too well, rendering it incapable of generating good predictions under new situations. As a result, testing the ANN model on a new dataset during the training process is crucial, first to check that the chosen structure gives outstanding results under random settings, and subsequently to fine-tune the structure choice. This inquiry will focus on one buried layer with 10 neurons.



**Fig 7:** ANN Model designation

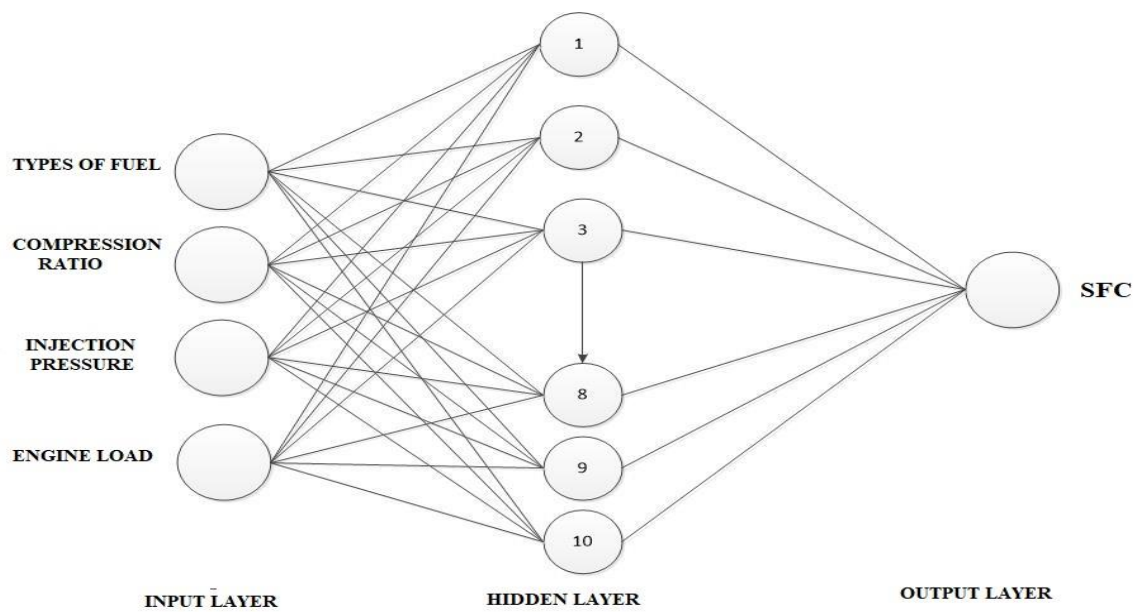


Fig 8: LM10TP model with 3 layers

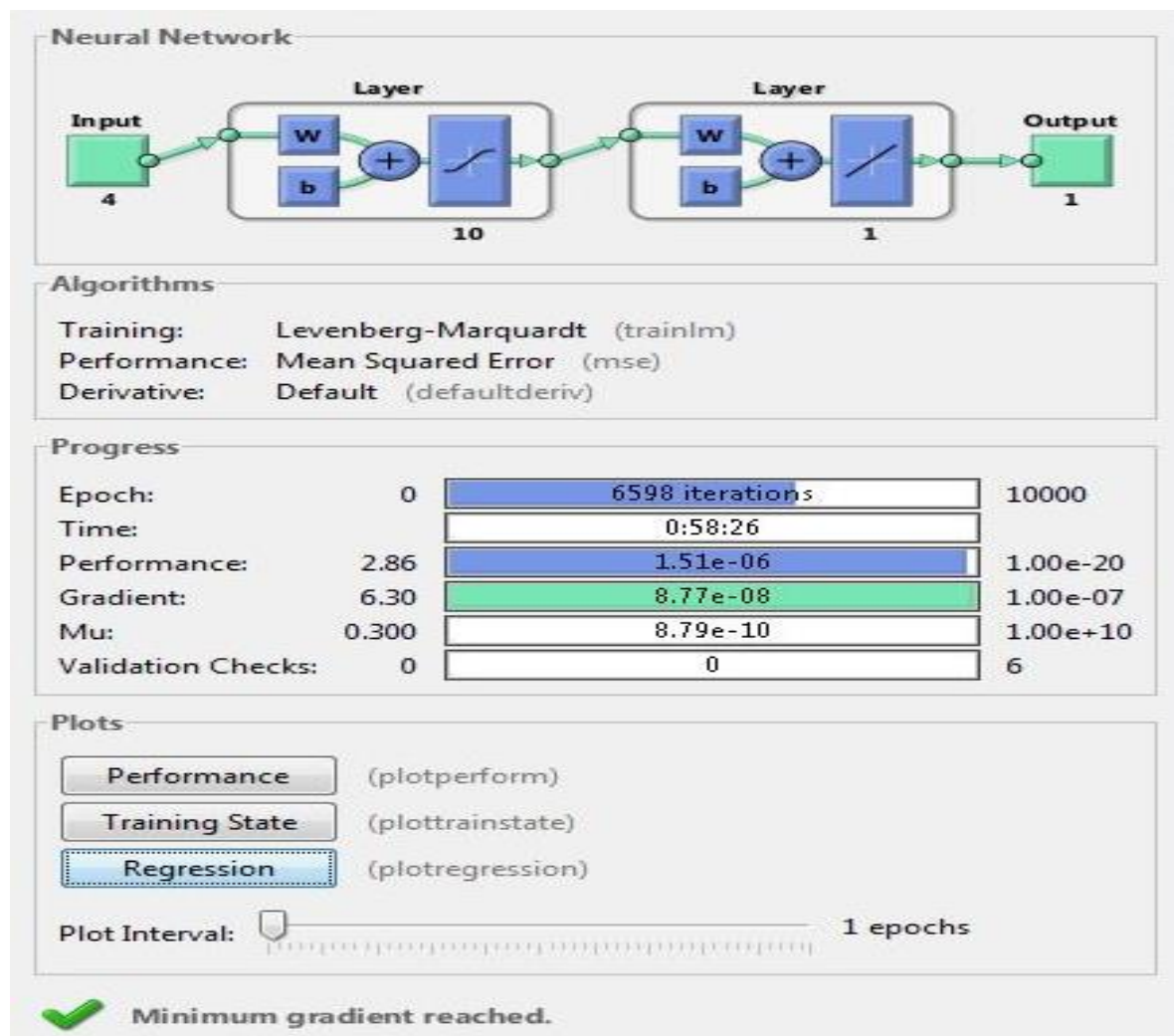


Fig 9: LM10TP model Training

Figure 7 depicts how this model was named. This term refers to the numerous properties of the produced ANN model. It goes through the many types of training methods that are utilised, as well as the amount of neurons in the hidden layer, the transfer function used between the input and hidden layers, and the transfer function used between the hidden and output layers. Finally, a three-layer ANN model was created, trained, and simulated: one input layer, one hidden layer, and one output layer. The number of neurons in the input and output layers remained constant at four and one, respectively. In this study, one hidden layer with 10 neurons used. In model, the tansig transfer function utilised between the hidden and input layers, while the purelin transfer function used between the output and hidden layers.

Following data normalisation, target data files and input data files are created for training. Following data normalisation, target data files and input data files are created for training. Target data files contain targets for training and validation data sets, which are normalised measured specific fuel consumption thresholds. Works includes a prediction challenge that required the end error to be reduced to a very minimal number. Figure 8 illustrates the LM10TP model's fundamental perspective, whereas Figure 9 depicts the LM10TP model's neural network training window.

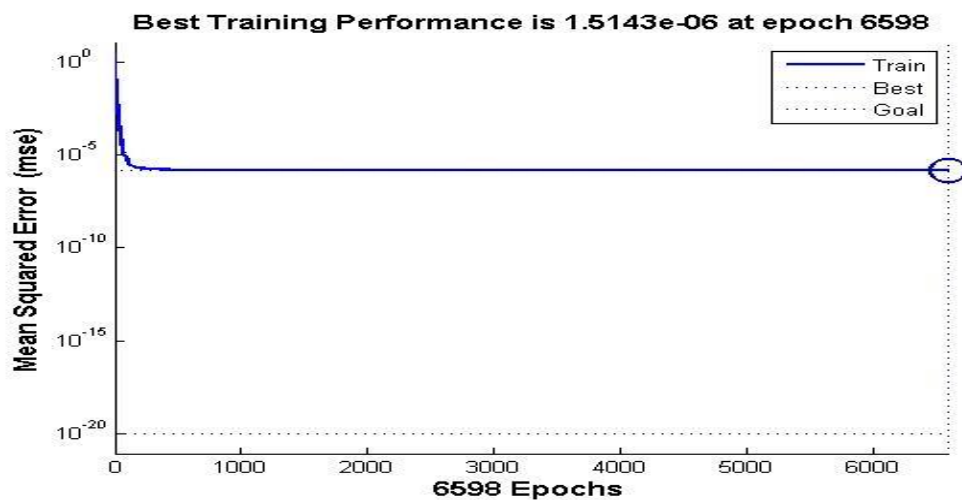


Fig 10: LM10TP model training performance graph

At epoch 6598, the best Training Performance is  $1.5143 \times 10^{-06}$ . The training performance (MSE) graph of the LM10TP model created during training is depicted in Figure 8. The training was stopped after 6598 epochs since the performance goal was attained. It is a great diagnostic tool for plotting faults and monitoring training progress.

## 8. Mathematical Model For Predicting Output

By modifying and storing suitable weights in the interconnection connections between neurons in different layers, the ANN model is trained. These weight values are the parameters responsible for allowing trained ANN models to forecast. The following equations 2 and 3 were utilised to generate the ANN output using weight, bias matrix, and transfer function.

For first layer output

$$a1 = f1 [(net. iw \{1, 1\} \times p) + (net. b1 \{1\})]. \quad (2)$$

For second layer output

$$a2 = f2 [(net. lw \{2, 1\} \times a1) + (net. b2 \{2\})], \quad (3)$$

where  $a1$  and  $a2$  are the hidden layer and output layer of output vectors.  $f1$  = tansig transfer function,  $f2$  = purelin transfer function,  $lw$  and  $iw$  are the weight matrices of the output and hidden layers,  $p$  is the input vector, and  $b1$  and  $b2$  are the bias vectors of the hidden and output layers, respectively.

**Table 6:** Weights in LM10TP model connections

Weight values					Bias Values	
Input–Hidden Layer				Hidden – Output layer	Input – Hidden layer	Hidden – Output layer
6.221514	3.123819	3.144247	2.875623071	-8.6675	2.178405713	3.26535687
14.4759	16.0651	-12.271	-34.12866049	0.173021	-29.1015509	
-3.33666	0.330777	2.196083	2.790147383	39.44371	9.59412524	
10.54957	-2.67429	-2.7649	-9.758369212	-0.04227	-2.26305401	
1.451752	1.972002	-1.72853	-6.588162804	-0.32879	-5.16054739	
-35.1262	-45.0384	6.259702	29.2926789	-0.00413	17.94165217	
-1.92107	0.539011	0.430859	3.65300448	-0.05577	0.501818928	
7.744301	3.116884	3.137591	2.832754193	-27.3696	3.18536946	
-0.03127	0.013652	0.05915	14.71766868	-43.8343	16.5848082	
7.220715	3.06043	3.08066	2.794263766	36.03121	2.892288716	

## 9. ANN Model Accuracy Checking

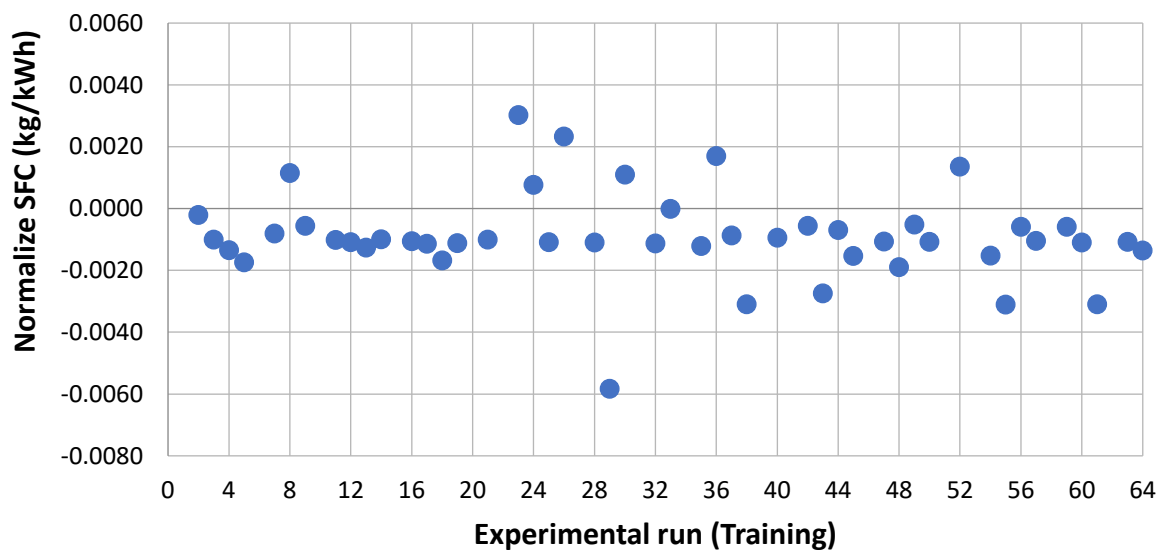
ANN is producing great predictions, test data that has never been fed into the network is used, and the results are analysed. MSE, RMSE & coefficient of multiple determination ( $R^2$ ) measurements were used for comparisons. The following equations 4, 5, and 6 are used to calculate these values:

$$MSE = \frac{1}{n} \sum_{i=1}^n (a_i - p_i)^2 \quad (4)$$

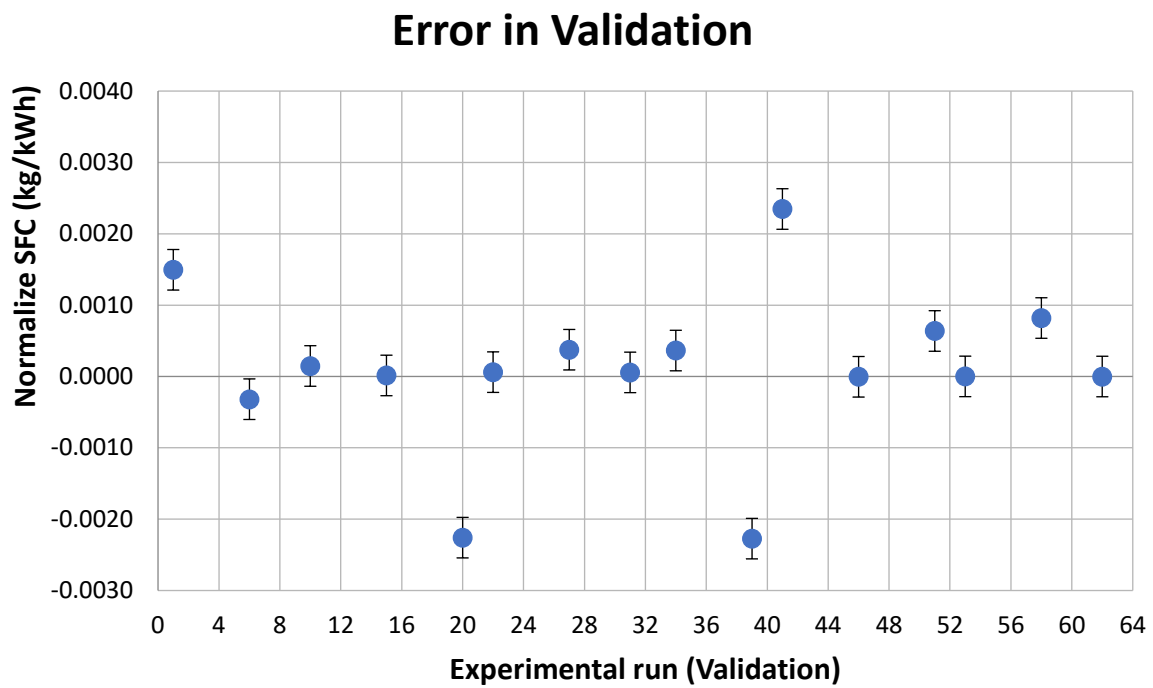
$$RMSE = \sqrt{\frac{1}{n} \sum_{i=1}^n (a_i - p_i)^2} \quad (5)$$

$$R^2 = 1 - \frac{\sum_{i=1}^n (a_i - p_i)^2}{\sum_{i=1}^n (p_i)^2} \quad (6)$$

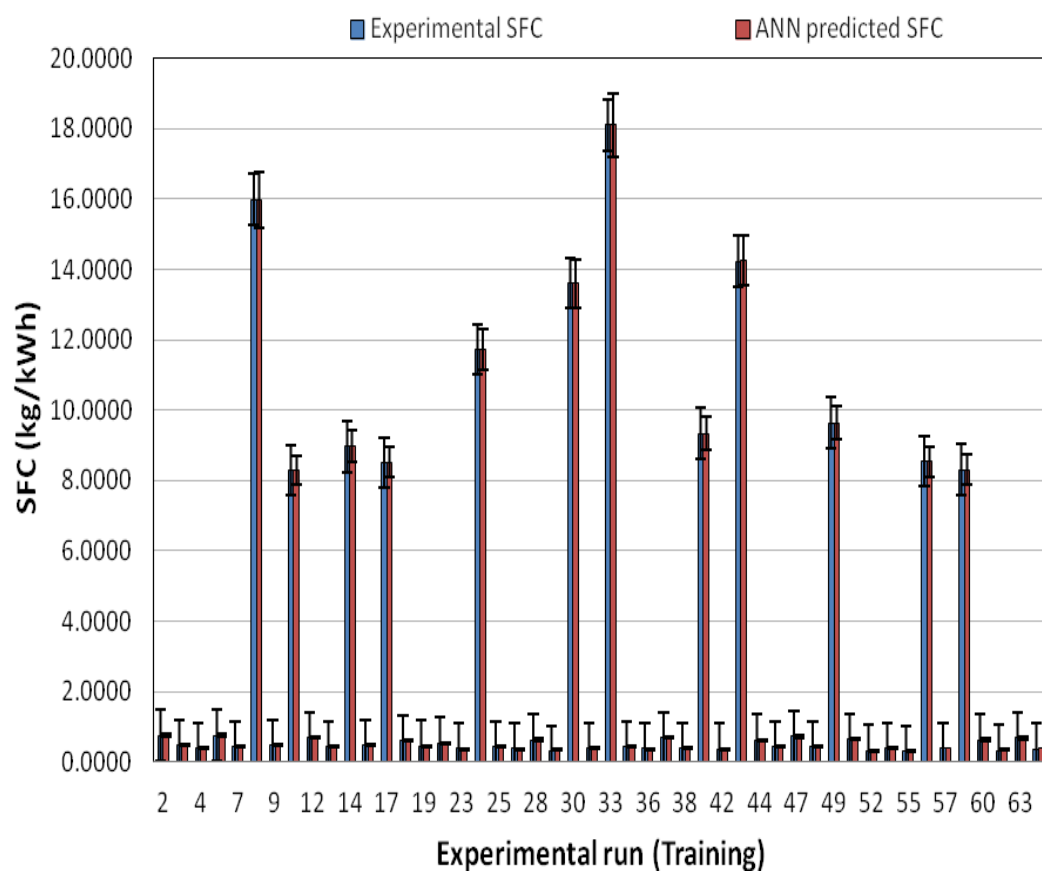
## Error in Training







**Fig 11:** LM10TP model prediction errors in Training and Validation



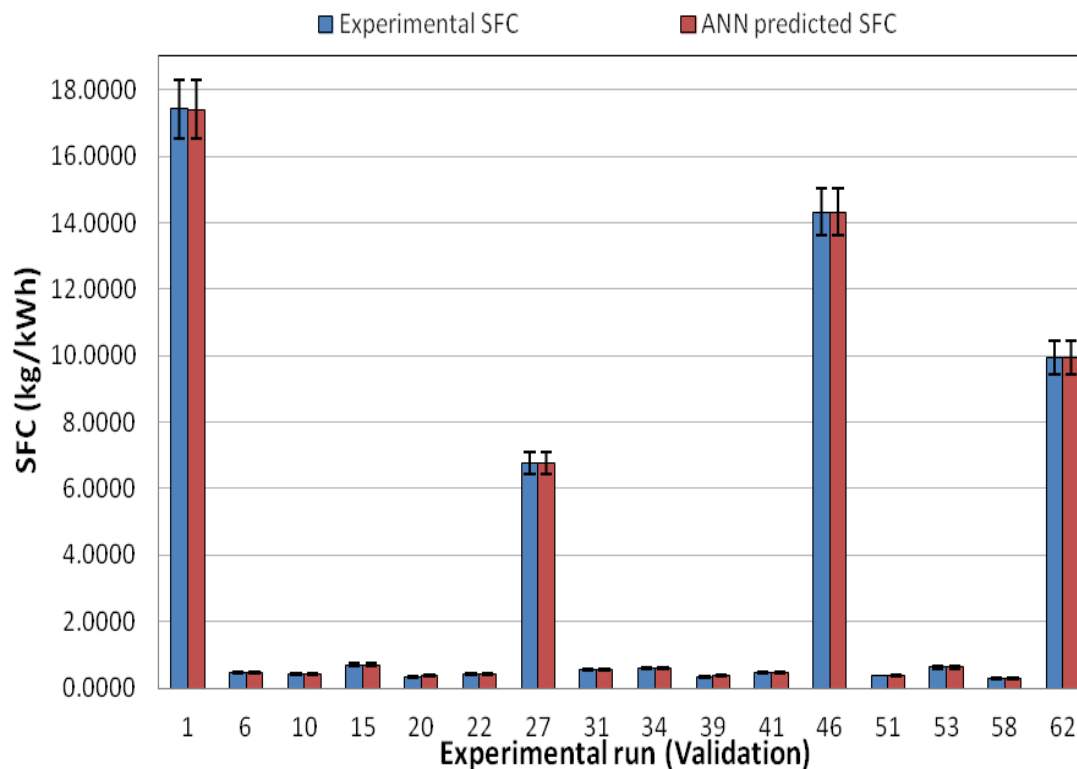


Fig 12: Actual vs. ANN predicted result in Training and Validation

The MATLAB programme was used to validate the prediction model's errors. The simulated ANN results were exported into the MATLAB workspace after training. Following the collection of training and experimental data, all findings were validated for three types of error terms. Figure 11 displays the LM10TP model's prediction errors throughout training and validation. In training, the LM10TP architecture's mean square error, root mean square error, and coefficient of determination  $R^2$  are  $1.5143 \times 10^{-06}$ , 0.0012, and 1, respectively. The MSE, RMSE & coefficient of determination  $R^2$  for the LM10TP architecture in the validation are  $1.2185 \times 10^{-06}$ , 0.0011, and 0.9999, respectively.

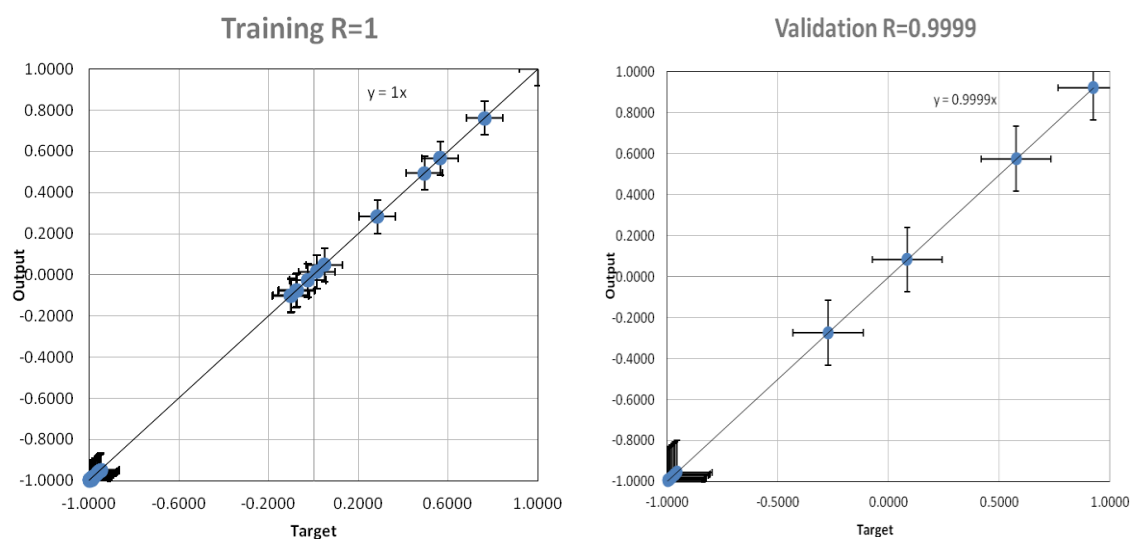


Fig 13: LM10TP Model Linear Fitting

It demonstrates that this model performed well in both training and validation for particular fuel consumption predictions. Figure 12 shows a comparison of the LM10TP model's anticipated fuel consumption with the actual target during training and validation. Different colors and markers are used to demonstrate the comparison. The graph clearly shows that ANN's projected outcomes are quite close to real aims. To some degree, the mistakes on the training and validation sets may be used to measure the performance of a trained network is usually beneficial to analyse the network response in higher depth. This analysis is performed by the routine postreg. Postreg was receiving the network output and the related objectives. It offered three options. The first 2 values, b & m, are the slope and y-intercept, respectively. It was carried out for training and validation purposes between the network outputs and the given targets. Figure 13 shows linear regression with three parameters m, b, and R for training and validation of the LM10TP model. Throughout training, R is equal to one, meaning that there is a perfect correlation between objectives and outputs. The validation graphs and parameters show that the LM10TP model fits linearly with  $R = 0.9999$ . This shows that the LM10TP model is ideally suited for precise fuel usage.

## 10. Multiple Linear Regression Analysis

Linear regression is a technique for describing the connection between a scalar dependent variable and one or more independent variables denoted by the letter X. When there is just one independent variable, simple linear regression is performed. When there are several independent variables, multiple linear regression is utilised. The relationship between a response variable ( $\hat{Y}$ ) and 3 predictor variables ( $X_1$ ,  $X_2$  &  $X_3$ ) is described by a multiple linear regression equation. Equation (7) shows the multiple regression.

$$\hat{Y} = B_0 - B_1 \cdot X_1 - B_2 \cdot X_2 - B_3 \cdot X_3, \quad (7)$$

Where:

$\hat{Y}$  - Predicted value of Specific fuel consumption,

$X_1$  – Compression Ratio,  $X_2$  – Injection Pressure,  $X_3$  - % of full load,

$B_0$  – Approximate value of y-intercept,

$B_1$ ,  $B_2$ , and  $B_3$  Approximate value of the autonomous variable coefficient.

**Table 7: MLR Analysis Table**

Term	Coef	SE Coef	T-Value	P-Value	VIF
Constant	11.27	8.84	1.28	0.209	1.01
CR	-0.132	0.459	-0.29	0.774	1.01
IP (bar)	-0.0040	0.0217	-0.18	0.856	1.02
Load (kg)	-0.817	0.115	-7.13	0.000	1.01
Types of fuel					
1	-0.017	0.885	-0.02	0.985	1.50
2	0.004	0.891	0.00	0.996	1.52
3	0.643	0.885	0.73	0.472	1.50

$$S = 3.53786, R\text{-sq} = 56.24\%, R\text{-sq(aj)} = 49.83\%, R\text{-sq(pred)} = 39.37\%$$

MLR analysis is performed using Minitab 16 software. Table 7 displays the results of the MLR analysis performed with Minitab. Relation of Specific fuel consumption with Compression Ratio, Injection Pressure and % of full load is shown in equation (8), (9), (10) and (11).

$$\text{Fuel-1, SFC (kg/kWh)} = 11.26 - 0.132 \text{ CR} - 0.0040 \text{ IP (bar)} - 0.817 \text{ Load (kg)} \quad (8)$$

$$\text{Fuel-2, SFC (kg/kWh)} = 11.28 - 0.132 \text{ CR} - 0.0040 \text{ IP (bar)} - 0.817 \text{ Load (kg)} \quad (9)$$

$$\text{Fuel-3, SFC (kg/kWh)} = 11.92 - 0.132 \text{ CR} - 0.0040 \text{ IP (bar)} - 0.817 \text{ Load (kg)} \quad (10)$$

$$\text{Fuel-4, SFC (kg/kWh)} = 10.64 - 0.132 \text{ CR} - 0.0040 \text{ IP (bar)} - 0.817 \text{ Load (kg)} \quad (11)$$

Because the p-value is less than 5%, Compression Ratio, Injection Pressure, and % of full load have a statistically significant influence on Specific fuel consumption at the 95% confidence level. Table 7 displays the R Square (56.24) and Adjusted R Square (49.83) values, demonstrating that the LM10TP ANN model outperforms the linear regression model in terms of prediction output. MLR model is developed to examine the versatility of ANN model. In this study we are comparing R2 and MSE error of both the model.

### 11. Comparison of ANN and MLR

Table 8 compares the ANN and MLR prediction models. The RMSE between the experimental and projected responses for the ANN and MLR models was 0.012 and 3.374, respectively. Both models predicted particular fuel consumption; however the ANN model outperformed the MLR model in forecasting the SFC. This might be because constructing a sustainable regression model requires a significant quantity of data, but the ANN can recognize associations with small data. The impact of the predictors on the response variable, which may or may not be linear, provides a second reason. Particularly, their superior aptitude and flexibility in modelling nonlinearity, ANN models are likely to estimate Specific fuel use with more accuracy. As a result, ANN may be favoured when there are less datasets.

**Table 8:** Comparison of MLR prophecy model and ANN error

Run	Experimental SFC (kg/kWh)	ANN Predicted SFC (kg/kWh)	ANN Error	ANN RMS Error	MLA Predicted SFC (kg/kWh)	MLA Error	MLA RMS Error
1	17.42	17.407	0.013	0.012	8.454	8.966	3.374
2	0.763	0.755	0.008		5.114	-4.351	
3	0.478	0.477	0.001		1.758	-1.280	
4	0.409	0.411	-0.002		-1.754	2.163	
5	0.764	0.77	-0.006		5.258	-4.494	
6	0.474	0.477	-0.003		1.624	-1.150	
7	0.441	0.439	0.003		-1.716	2.157	
8	15.984	15.973	0.011		8.082	7.902	
9	0.481	0.477	0.005		1.678	-1.197	
10	0.421	0.419	0.001		-1.858	2.278	
11	8.287	8.291	-0.004		7.948	0.339	
12	0.709	0.709	0		4.608	-3.899	
13	0.439	0.44	-0.002		-1.844	2.283	
14	8.964	8.967	-0.004		7.896	1.067	
15	0.706	0.706	0		4.556	-3.850	
16	0.474	0.474	0		1.208	-0.734	
17	8.507	8.512	-0.005		8.392	0.115	
18	0.619	0.624	-0.005		5.028	-4.409	
19	0.464	0.464	0		1.655	-1.191	
20	0.344	0.364	-0.02		-1.652	1.996	
21	0.543	0.542	0.001		5.000	-4.458	
22	0.412	0.412	0.001		1.742	-1.330	
23	0.4	0.363	0.037		-1.777	2.177	
24	11.731	11.721	0.01		8.069	3.662	

25	0.446	0.446	0	1.592	-1.146
26	0.393	0.362	0.03	-1.911	2.304
27	6.771	6.767	0.003	7.960	-1.189
28	0.637	0.637	0	4.702	-4.065
29	0.321	0.364	-0.042	-1.890	2.211
30	13.604	13.591	0.012	7.998	5.606
31	0.567	0.567	0.001	4.486	-3.919
32	0.403	0.403	0	1.236	-0.834
33	18.094	18.094	0	9.122	8.972
34	0.604	0.601	0.003	5.717	-5.112
35	0.441	0.442	-0.001	2.418	-1.977
36	0.395	0.37	0.025	-0.996	1.391
37	0.708	0.706	0.002	5.632	-4.924
38	0.394	0.411	-0.018	2.317	-1.923
39	0.35	0.37	-0.02	-1.162	1.512
40	9.334	9.338	-0.004	8.660	0.674
41	0.488	0.467	0.021	2.183	-1.695
42	0.375	0.37	0.005	-1.181	1.556
43	14.221	14.243	-0.022	8.682	5.540
44	0.627	0.623	0.003	5.211	-4.584
45	0.44	0.444	-0.004	-0.759	1.200
46	14.322	14.322	0	8.621	5.701
47	0.729	0.729	0	5.282	-4.553
48	0.453	0.461	-0.007	1.868	-1.415
49	9.633	9.633	0	7.752	1.881
50	0.657	0.657	0	4.486	-3.829
51	0.4	0.395	0.006	1.048	-0.647
52	0.33	0.308	0.022	-2.186	2.515
53	0.63	0.63	0	4.352	-3.723
54	0.388	0.392	-0.004	1.094	-0.706
55	0.317	0.335	-0.018	-2.417	2.734
56	8.545	8.545	0	7.356	1.189
57	0.384	0.384	0	0.952	-0.568
58	0.307	0.3	0.007	-2.143	2.450
59	8.312	8.312	0	7.320	0.992
60	0.633	0.633	0	3.972	-3.339
61	0.328	0.346	-0.018	-2.350	2.678
62	9.948	9.948	0	7.301	2.647
63	0.69	0.69	0	4.059	-3.369
64	0.381	0.383	-0.002	0.515	-0.134

## 12. Conclusion

The current study intended to create an Experimental-ANN hybrid model for particular fuel consumption of a Compression Ignition Engine. Based on L64 orthogonal array the ANN model of SFC prepared. The ANN model for predicting particular fuel use comes to the following findings.

Neural network model based on experimental result decrease the Time and efforts.

In training, the mean square error and coefficient of determination for the LM10TP architecture are  $1.5143 \times 10^{-6}$  and 1, respectively.

In the validation, the MSE and coefficient of determination for the LM10TP design are  $1.2185 \times 10^{-6}$  and 0.9999, respectively.

The ANN's projected specific fuel consumption values are extremely similar to the experimental data.

As a consequence, Utilized ANN is best substitute for predicting particular fuel consumption based on the impacts of Compression Ignition Engine settings.

## Acknowledgement

The authors would like to thank LDRP Institute of Technology and Research, Gandhinagar, Gujarat, India for providing Diesel Engine for Experimental work.

## References

- [1] Cheikh, Kezrane, Awad Sary, Loubar Khaled, Liazid Abdelkrim, and Tazerout Mohand. "Experimental assessment of performance and emissions maps for biodiesel fueled compression ignition engine." *Applied energy* 161 (2016): 320-329.
- [2] Ma, Yinjie, Ronghua Huang, Jianqin Fu, Sheng Huang, and Jingping Liu. "Development of a diesel/biodiesel/alcohol (up to n-pentanol) combined mechanism based on reaction pathways analysis methodology." *Applied Energy* 225 (2018): 835-847.
- [3] Dey, S., M. Deb, and P. K. Das. "An investigation of diesohol-biodiesel mixture in performance-emission characteristics of a single cylinder diesel engine: A trade-off benchmark." *International Journal of Automotive and Mechanical Engineering* 16, no. 4 (2019): 7464-7479.
- [4] Shahir, S. A., H. H. Masjuki, M. A. Kalam, A. Imran, IM Rizwanul Fattah, and Ahmed Sanjid. "Feasibility of diesel–biodiesel–ethanol/bioethanol blend as existing CI engine fuel: An assessment of properties, material compatibility, safety and combustion." *Renewable and Sustainable Energy Reviews* 32 (2014): 379-395.
- [5] Parlak, Adnan, Yasar Islamoglu, Halit Yasar, and Aysun Egrisogut. "Application of artificial neural network to predict specific fuel consumption and exhaust temperature for a diesel engine." *Applied Thermal Engineering* 26, no. 8-9 (2006): 824-828.
- [6] Wang, Saerom, Ksenia Kirillova, and Xinran Lehto. "Travelers' food experience sharing on social network sites." *Journal of Travel & Tourism Marketing* 34, no. 5 (2017): 680-693.
- [7] Tosun, Erdi, Kadir Aydin, and Mehmet Bilgili. "Comparison of linear regression and artificial neural network model of a diesel engine fueled with biodiesel-alcohol mixtures." *Alexandria Engineering Journal* 55, no. 4 (2016): 3081-3089.
- [8] Pai, P. Srinivasa, and BR Shrinivasa Rao. "Artificial neural network based prediction of performance and emission characteristics of a variable compression ratio CI engine using WCO as a biodiesel at different injection timings." *Applied Energy* 88, no. 7 (2011): 2344-2354.
- [9] Ghobadian, Barat, Talal Yusaf, Gholamhasan Najafi, and Mahdi Khatamifar. "Diesterol: an environment-friendly IC engine fuel." *Renewable Energy* 34, no. 1 (2009): 335-342.
- [10] Oğuz, Hidayet, Ismail Saritas, and Hakan Emre Baydan. "Prediction of diesel engine performance using biofuels with artificial neural network." *Expert Systems with Applications* 37, no. 9 (2010): 6579-6586.
- [11] Javed, Syed, YVV Satyanarayana Murthy, Rahmath Ulla Baig, and D. Prasada Rao. "Development of ANN model for prediction of performance and emission characteristics of hydrogen dual fueled diesel engine with Jatropa Methyl Ester biodiesel blends." *Journal of Natural Gas Science and*



- Engineering 26 (2015): 549-557.
- [12] Roy, Sumit, Ajoy Kumar Das, Vivek Singh Bhadouria, Santi Ranjan Mallik, Rahul Banerjee, and Probir Kumar Bose. "Adaptive-neuro fuzzy inference system (ANFIS) based prediction of performance and emission parameters of a CRDI assisted diesel engine under CNG dual-fuel operation." *Journal of Natural Gas Science and Engineering* 27 (2015): 274-283.
- [13] Bhowmik, Subrata, Rajsekhar Panua, Durbadal Debroy, and Abhishek Paul. "Artificial neural network prediction of diesel engine performance and emission fueled with diesel–kerosene–ethanol blends: a fuzzy-based optimization." *Journal of Energy Resources Technology* 139, no. 4 (2017).
- [14] Patel, Tushar M., and Nilesh M. Bhatt. "Development of FEA-ANN hybrid model for equivalent stress prediction of automobile structural member." *Automatic Control and Computer Sciences* 50, no. 5 (2016): 293-305.
- [15] Srinidhi, C., A. Madhusudhan, and S. V. Channapattana. "Parametric studies of CI engine at various injection strategies using biodiesel blended nanoparticles as fuel." *International Journal of Ambient Energy* 43.1 (2022): 117-127.
- [16] Srinidhi, C., A. Madhusudhan, and S. V. Channapattana. "Comparative analysis of exhaust gas recirculation and nanoparticles on the performance and emission of diesel engine fuelled with Neem biodiesel blend." *International Journal of Ambient Energy* 43.1 (2022): 290-299.
- [17] Srinidhi, Campli, et al. "Comparative investigation of performance and emission features of methanol, ethanol, DEE, and nanopartilces as fuel additives in diesel-biodiesel blends." *Heat Transfer* 50.3 (2021): 2624-2642.
- [18] Srinidhi, Campli, et al. "RSM based parameter optimization of CI engine fuelled with nickel oxide dosed Azadirachta indica methyl ester." *Energy* 234 (2021): 121282.
- [19] Campli, Srinidhi, et al. "The effect of nickel oxide nano-additives in Azadirachta indica biodiesel-diesel blend on engine performance and emission characteristics by varying compression ratio." *Environmental Progress & Sustainable Energy* 40.2 (2021): e13514.
- [20] Channapattana, S. V., Abhay A. Pawar, and Prashant G. Kamble. "Optimisation of operating parameters of DI-CI engine fueled with second generation Bio-fuel and development of ANN based prediction model." *Applied energy* 187 (2017): 84-95.
- [21] Channapattana, S. V., Abhay A. Pawar, and Prashant G. Kamble. "Effect of injection pressure on the performance and emission characteristics of VCR engine using honne biodiesel as a fuel." *Materials Today: Proceedings* 2.4-5 (2015): 1316-1325.
- [22] Channapattana, S. V., Abhay A. Pawar, and Prashant G. Kamble. "Performance and emission characteristics of CI-DI VCR engine using honne oil methyl ester." *IOSR J Mech Civil Eng (IOSRJMCE)* (2015): 2278-1684.